Earthq Eng & Eng Vib (2015) 14: 503-516 **DOI**:10.1007/s11803-015-0040-3

Effect of types of reinforcement on plastic hinge rotation parameters of RC beams under pushover and cyclic loading

V. V. S. Surya Kumar Dadi[1†] and Pankaj Agarwal[2‡]

1. *Department of Civil Engineering, Institute of Technology, Guru Ghasidas Vishwavidyalaya, Bilaspur* (*C.G.*)*, India*

2. *Department of Earthquake Engineering, Indian Institute of Technology Roorkee, Roorkee* (*UK*)*, India*

Abstract: Experimental evaluation of reinforced concrete beam specimens with different characteristics of reinforcement subjected to pushover and cyclic loading is presented. Plastic hinge rotation parameters are determined based on the idealization of pushover and hysteresis curves of reinforced concrete beam specimens constructed in two percentage of reinforcement (0.471% and 0.71%) with different ductile characteristics. The experimental test results provide a clear demarcation of the effect of types of loading and the types of reinforcement on the nonlinear performance characteristics of beam specimens. These results are helpful to update the nonlinear modeling parameters of beam components for the specific type of reinforcement used in the construction of a structure. The updated non-linear modeling parameters of beam components in lumped plasticity model are compared with the values of ASCE/SEI 41-06 (2007) used for the performance based design of structures.

Keywords: concrete structures; pushover loads; cyclic loads; hysteresis behavior; plastic rotation; non-linear modeling parameters; reinforcing steels.

1 Introduction

Precise evaluation of nonlinear modeling parameters of components is important for predicting the non-linear response of any reinforced concrete structure. The modeling accuracy depends upon the representative material models by which the components are actually composed. Analytical predictions of plastic rotations are very challenging and are only appropriate if the characteristics of constituent materials are experimentally evaluated and validated ranging from material testing to their component behavior. Deformation capacities of components vary with the types and amount of reinforcement. The ASCE/SEI 41-06 (2007) provides the moment-rotation parameters of beam component under different modes of failure based on tension and compression reinforcement, condition of confinement and shear strength. The nonlinear modeling parameters specific to reinforcement type as a component have not been prevalent in ASCE/SEI 41-06 (2007).

The various types of reinforcing bars used as a constructional material possess different characteristics such as brittle, ductile and highly ductile. It is necessary to study the effect of the reinforcement characteristics on the nonlinear behavior of components. Evaluation of specific plastic rotation capacity of a specific type of reinforcement component is necessary for proper representation of the specific non-linear deformation capacity. In this regard, experimental evaluation proves to be the best means to determine the comparative performances of a component involving varied constituents under cyclic loading. There is limited number of studies available on beam tests under cyclic loading and pushover for comparison. Experimental and analytical studies on beam components carried out in the past are limited to one specific type of reinforcement (Iyengar *et al.*, 1972; Hwang and Scribner, 1984; Darwin and Nmai, 1986; Marfia *et al.*, 2004; Fantilli *et al.*, 2005; Oehlers *et al.*, 2005; Scott and Whittle, 2005; Inel and Ozmen, 2006; Caripinteri *et al.*, 2009; Haskett *et al.*, 2009; Marefat *et al.*, 2009; Melo *et al.*, 2011). This paper presents two types of reinforcement with different characteristics. The results demonstrate the effect of type of reinforcement and type of loading on the non-linear behavior of components. These results are useful for updating the lumped plasticity models under pushover analysis as per ASCE/SEI 41-06 (2007).

2 Comparative study of reinforcing bars based on uni-axial and cyclic tests

Reinforcements with different characteristics are

Correspondence to: Pankaj Agarwal, Department of Earthquake Engineering, Indian Institute of Technology Roorkee, Roorkee (UK), India
Tel: +91-01332-285317; Fax: +91-01332-285317
E-mail: panagfeq@gmail.com
†Assistant Professor; ‡Professor

Received August 25, 2013; **Accepted** July 18, 2014

used in the preparation of beam specimens, namely, (i) twisted ore reinforcement (TOR) also called high yield strength deformed (HYSD) reinforcement and (ii) thermo mechanically treated (TMT) reinforcement. In this study, TMT reinforcement is obtained from two different sources, namely, from a leading manufacturing agency known as STMT reinforcement and second is from a local agency known as LTMT reinforcement. The TOR reinforcement is generally used in past construction while TMT reinforcement is widely used in recent reinforced concrete (RC) construction. Monotonic and cyclic behaviors of these types of reinforcement have been studied with the aim to highlight the effect of reinforcement characteristics on structural performance. The performance of different types of reinforcements under uni-axial tensile and cyclic test at different strain rates is shown in Fig. 1(a) and comparative performance of STMT and TOR type of reinforcement is shown in Fig. 1(b).

The TMT reinforcement demonstrates higher strength with more deformation over the TOR reinforcement. An approximately quantifiable increase in deformity of about 50% is observed in case of TMT reinforcement as compared to TOR reinforcement. Also a specific yield point is not observed in case of TOR reinforcement as compared with TMT reinforcement. The observed mode of failure of TMT reinforcement is necking before fracture and hence show maximum possible ductile behaviors. The increase in fracture strain energy of TMT reinforcement is about 70% over TOR reinforcement.

The hysteresis curves of TMT reinforcement show improvement in resisting more cycles compared to TOR type reinforcement within similar strain-amplitude loading up to fracture. The comparative cyclic strength decay curves clearly distinguish the individual performances of the TMT and TOR reinforcement. A degradation of (≈ 25%) in tension side and (≈ 45%) in compression side occurs in the second cycle of both the reinforcements. From 3rd cycle onwards, up to the points of initiation of fracture, the strength degradation decreased and is more or less the same for both reinforcement types and also on both the tension and compression sides of loading (≈ starting from 20% and up to 2%). This shows that under cyclic type of loading,

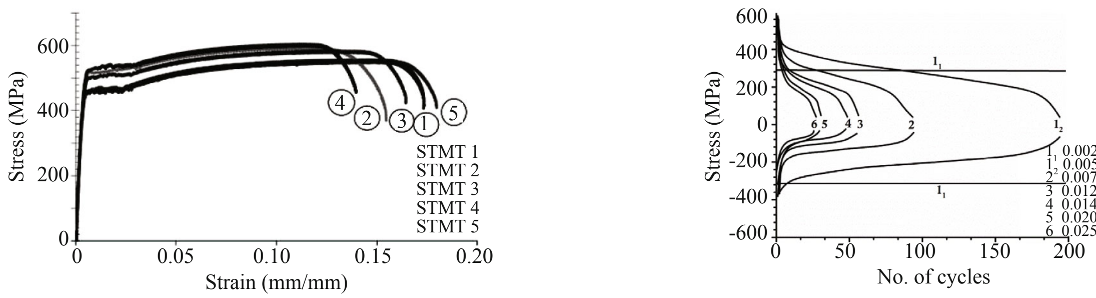

Monotonic stress-strain curves and strength decay plot of STMT reinforcement

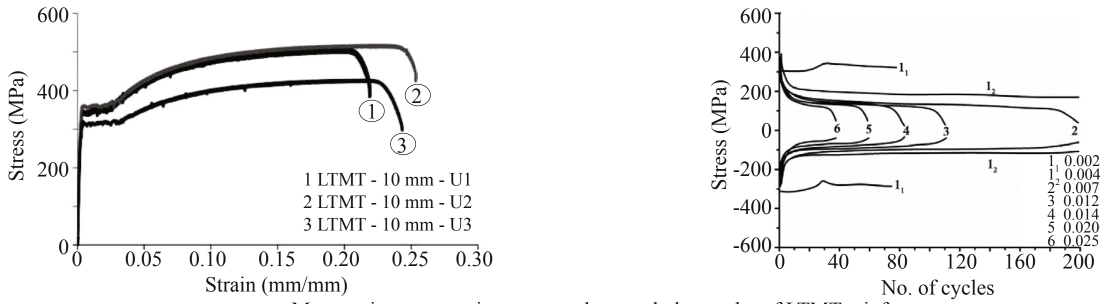

Monotonic stress-strain curves and strength decay plot of LTMT reinforcement

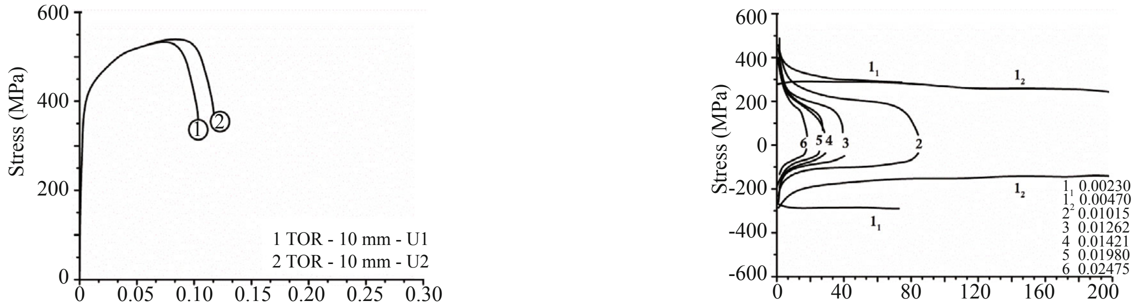

Monotonic stress-strain curves and strength decay plot of TOR reinforcement

Fig. 1(a) Performance evaluation of 10 mm reinforcing bar specimens of (a) STMT (b) LTMT (c) TOR under uni-axial tensile and cyclic test results

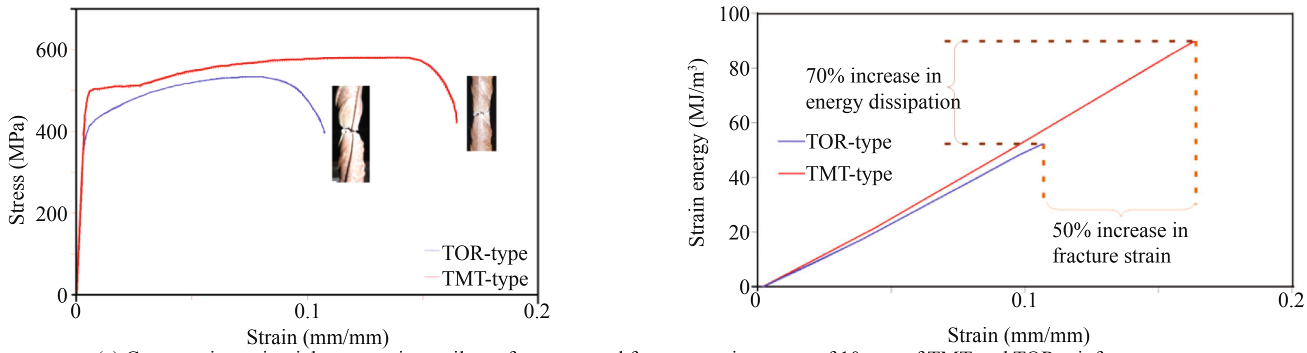

(a) Comparative uni-axial monotonic tensile performance and fracture strain energy of 10 mm of TMT and TOR reinforcement

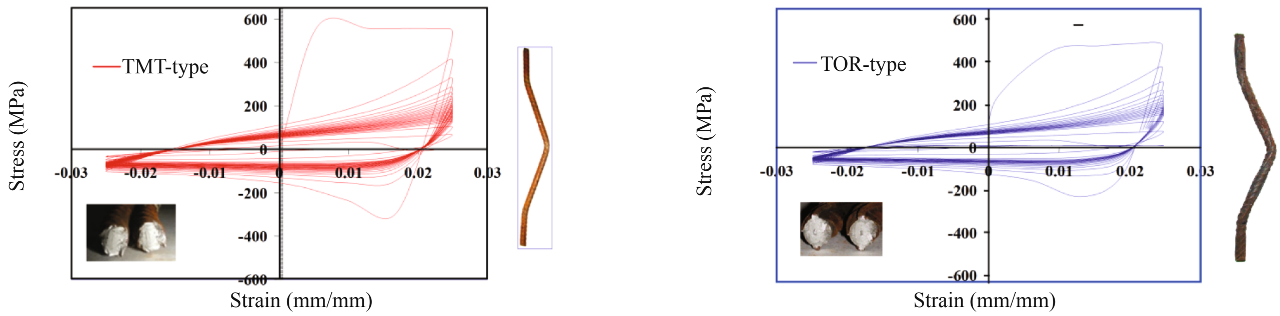

(b) Typical cyclic test results of 10 mm reinforcing bar specimens of TMT and TOR reinforcement type at strain of 0.025 with modes of failures

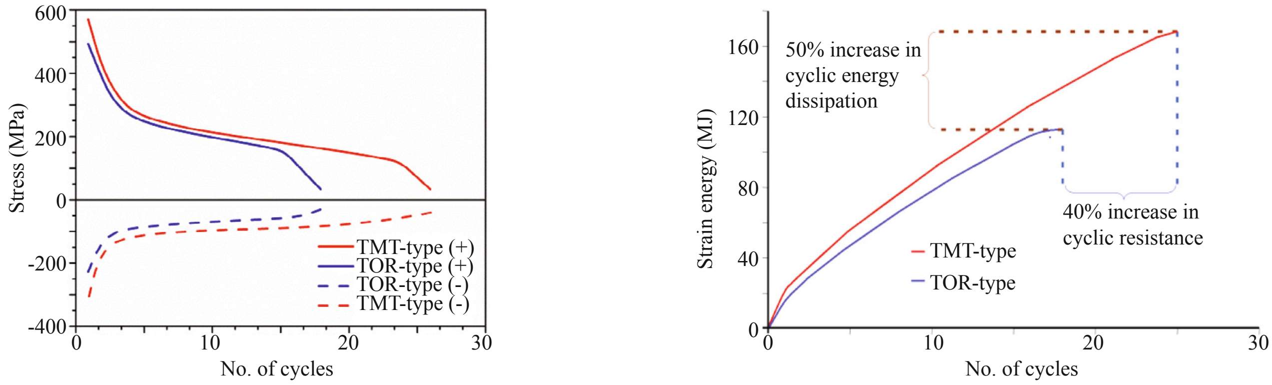

(c) Comparative cyclic performance in terms of strength decay and fracture strain energy of 10 mm TMT and TOR reinforcement at 0.025cyclic test strain

Fig. 1(b) Comparative performance of 10 mm of STMT and TOR reinforcement under uni-axial tensile and cyclic tests

the initial leg (i.e. 1st cycle to 2nd cycle), last leg (i.e. after initiation of cracking to the point of fracture) and the intermediate leg (the cycles between first and last legs) have similar trends of degradation, and in case of TMT reinforcement there is increased degradation in the intermediate legs than the TOR reinforcement. What is significant is that TMT reinforcement gives an increase in fracture strain energy of about 50% with an approximate quantifiable increase in deformity of about 40% as compared to TOR reinforcement. This trend is also observed in monotonic loading.

3 Pushover and cyclic performance evaluation of beam specimens with different characteristics of reinforcing bars

In total, twelve beam specimens with span to effective depth ratio (l/d) of 6.5 (S BEAM) have been tested under quasi-static loading in displacement control. These beam specimens are cast in two types of reinforcement, namely, TMT and TOR. The reinforcement details of these beam specimens are shown in Fig. 2. The actual sizes are 275 mm × 275 mm × 1.78 m reinforced with the same percentage of tension steel ρ ($\rho = A_s/b{\cdot}d$), where A_s is the area of bars in tension, b is the width and d is the effective depth of the section with cover of concrete 25 mm on both the faces in all the beams. Two variations in the quantity of tension reinforcement (0.47% and 0.71%) have been adopted for each type of reinforcement. The size of beam specimens and % of reinforcement are designed as per IS 13920: 1993 on the basis of minimum practical size dimension and failure in flexure, i.e., under-reinforced beam. The % of reinforcement varies on the basis of minimum ($\rho_{min} = 0.24 \frac{\sqrt{f_{ck}}}{f_y}$) and maximum ($\rho_{max}$ = 2.5%) % of reinforcement as recommended in IS 13920 (1993). All the beam specimens are cast in same aggregate, sand and

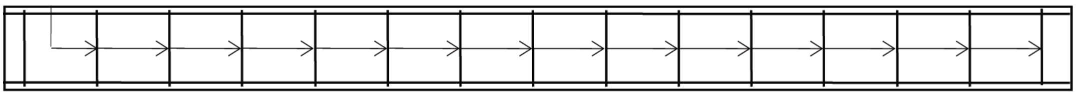

(a) Shear reinforcement detailing

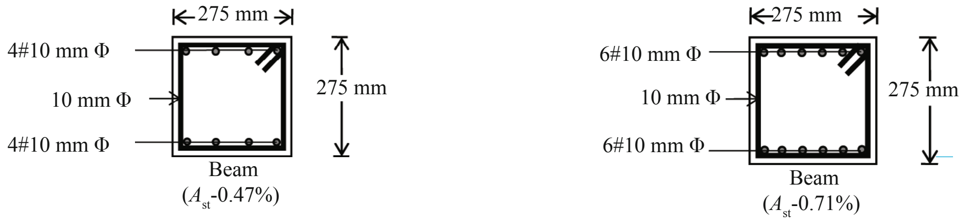

(b) Flexure reinforcement detailing with concrete cover of 25 mm

Fig. 2 Reinforcement details in beam specimens (a) shear reinforcement and (b) flexure reinforcement

cement ratio under similar environmental conditions to maintain uniform characteristic strength of concrete f_c (around 25 MPa). The pushover and cyclic performances of beam specimens have been evaluated under three different cases based on types of reinforcement i.e. (i) STMT (ii) LTMT and (iii) TOR.

The beam tests are carried out in simply supported conditions under pushover loading and cyclic loading. The tests have been carried out in the quasi-static testing facility. The salient features of the test set-up are; (i) *Strong Floor* (ii) *Reaction Wall*, (iii) *Two Servo-Hydraulic Actuators* with inbuilt, linearly varying displacement transducers (LVDTs) and load cells, with capabilities to displacement control as well as synchronization and (iv) *Two Mechanical Jacks,* as shown in Fig. 3.

The loading history is the ramp displacement with gradual increase in displacement amplitude under pushover loading whereas cyclic loading consists of sine waves with two cycles of equal displacement and increasing amplitudes in subsequent cycles at a very low frequency (f = 0.0083 Hz), starting from 5 mm cycle onwards with an increment of 5 mm. Test results of load-deformation up to failure under both types of testing for all specimens are presented. Since two actuators (A1, A2) are used for application of load, the resultant load (F) is the sum of the actuator loads while the resultant displacement (δ) is the average of actuator displacements as shown in Fig. 4.

The test results of all the beam specimens under pushover and cyclic testing are summarized in Table 1. The evaluated parameters for the beam specimens are: (a) flexural capacity of beams i.e. yield capacity (F_y) and ultimate capacity (F_u), (b) over strength factor (F_u/F_y), (c) displacement ductility level μ_L = (δu(i)/δy(i)) and displacement ductility μ = (δ_u /δ_y) and finally (d) energy dissipation (area under load deformation curve or cumulative area of load-deformation cycles. The specimens are evaluated to quantify the differences caused by the type of reinforcement or loading on the basis of these parameters. The experimentally evaluated ductility of beams reinforced with two typical reinforcement types (TOR as "1" and TMT as "2")

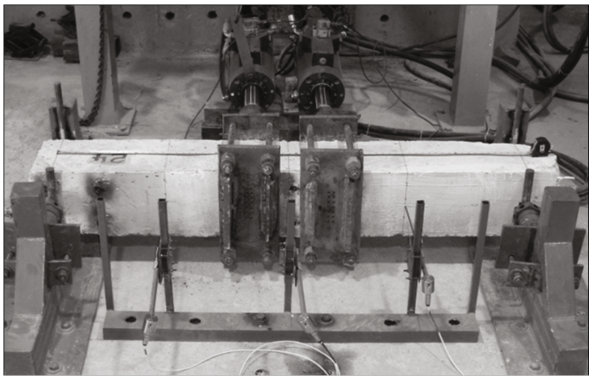

(a) Actual beam specimen under test

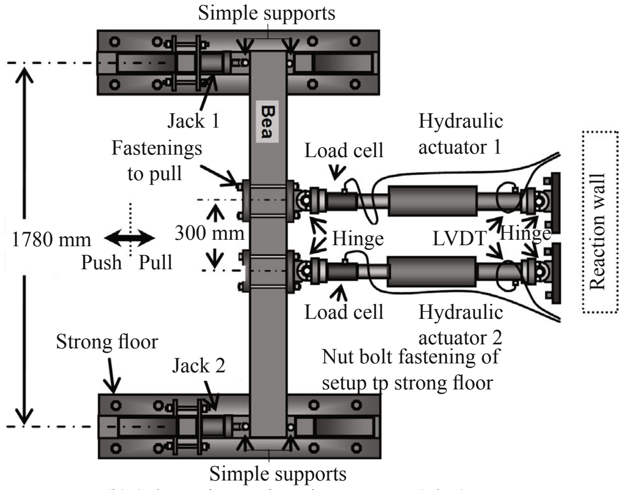

(b) Schematic quasi-static test setup (Plan)

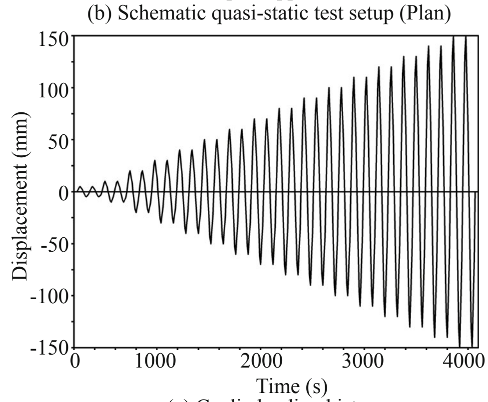

(c) Cyclic loading history

Fig. 3 Typical beam specimen under pushover and cyclic test

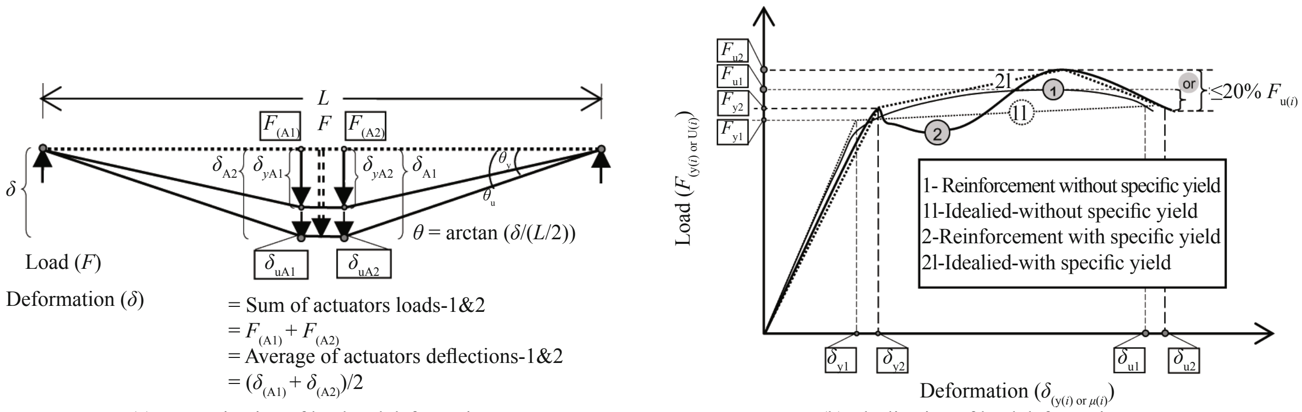

(a) Determination of load and deformation (b) Idealization of load deformation curves

Fig. 4 Idealization of envelope of pushover or cyclic curve of beam specimens with different types of reinforcement

Table 1 Test results of beam specimens with different types of reinforcement under pushover and cyclic loading

Sl. No.	Specimen ID	Test type/ A_{st} (%)	Moment (kN·m)		Over-strength factor		Ductility at % of ultimate load cycles	Energy dissipated (kN·m)	
			Yield	Ult.				Cycles	Envelop
	Short beam (SBEAM) specimens with 10 mm STMT reinforcement								
1	“SBEAM-01”	Pushover/0.47	37.14	41.89	1.13	C	08.0 @ 80%	-	4.80
2	“SBEAM-02”	Pushover/0.71	50.84	59.07	1.16	C	07.0 @ 98%	-	7.00
3	“SBEAM-03”	Cyclic/ 0.47	37.81	42.96	1.14	T	03.2 @ 98.7%	11.2	2.70
						C	03.3 @ 90.8%	9.5	2.00
4	“SBEAM-04”	Cyclic/ 0.71	53.03	56.30	1.06	T	03.0 @ 81%	36.2	6.30
						C	03.0 @ 91%	34.9	6.80
	Short beam (SBEAM) specimens with 10 mm LTMT reinforcement								
5	“SBEAM-05”	Pushover/0.47	21.03	31.33	1.49	C	22.6 @ 87.3%	-	5.80
6	“SBEAM-06”	Pushover/0.71	47.44	53.52	1.13	C	07.9 @ 99.0%	-	7.00
7	“SBEAM-07”	Cyclic/ 0.47	21.26	29.85	1.40	T	07.8 @ 99.1%	17.6	2.5
						C	07.7 @ 98.8%	16.9	2.4
8	“SBEAM-08”	Cyclic/ 0.71	30.88	41.08	1.33	T	05.0 @ 98.6%	17.4	2.8
						C	06.7 @ 84.6%	16.2	2.6
	Short beam (SBEAM) specimens with 10 mm TOR reinforcement								
9	“SBEAM-9”	Pushover/0.47	36.70	41.06	1.12	C	06.8 @ 99.2%	-	3.8
10	“SBEAM-10”	Pushover/0.71	39.83	48.78	1.22	C	02.3* @ 100% (up to 6.5)	-	1.2* (up to 2.3)
11	“SBEAM-11”	Cyclic/ 0.47	31.55	34.75	1.10	T	03.9 @ 99.3%	5.8	2.0
						C	02.7 @ 97.7%	4.0	1.2
12	“SBEAM-12”	Cyclic/ 0.71	42.96	50.97	1.19	T	04.7 @ 100%	15.0	3.4
						C	04.4 @ 97.4%	16.3	3.2

Note: T, C represents tension side and compression sides respectively, * indicates insufficient data

is based on the idealization of characteristic load-deformation envelope curves of pushover as well as cyclic tests as shown in Fig. 4. The post elastic strength degradation over yield ($F_{Deg\%}$) and post elastic stiffness degradation over yield stiffness ($K_{Deg\%}$) is given in Eqs. (1) and (2).

$$F_{Deg\%} = (1-(F-F_y)/F_y)\times 100 \tag{1}$$

$$K_{Deg\%} = \left[(1-(K-K_y)/K_y)\right]\times 100 \tag{2}$$

The pushover test results of beam specimens with STMT reinforcement are shown in Figs. 5(a) and 5(b). The typical behavior of specific yield type reinforcement

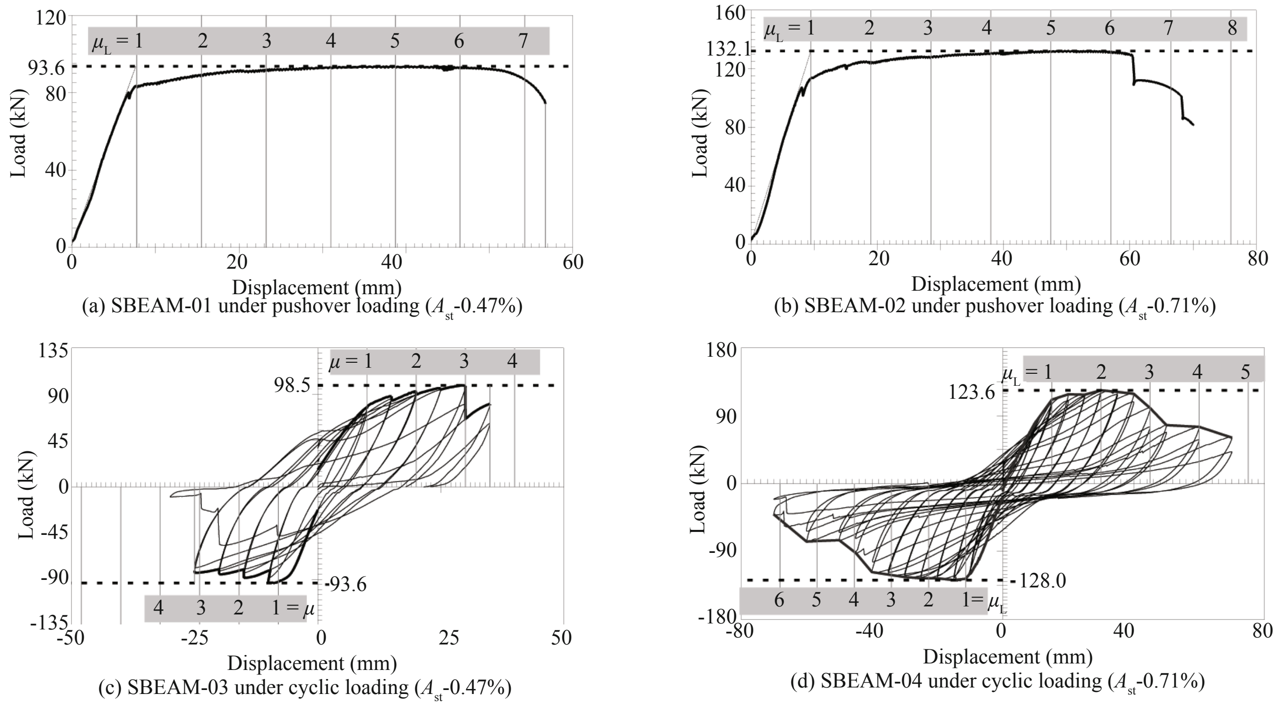

(a) SBEAM-01 under pushover loading (A_{st}-0.47%)
(b) SBEAM-02 under pushover loading (A_{st}-0.71%)
(c) SBEAM-03 under cyclic loading (A_{st}-0.47%)
(d) SBEAM-04 under cyclic loading (A_{st}-0.71%)

Fig. 5 Pushover and cyclic performance of beam specimens with STMT reinforcement

is observed in both sets of results with a clear appearance of yield point. A ductility level of greater than 7 is observed. The resulting failure is in the form of major flexural cracks below the loading face and finally leading to fracture of reinforcing bars giving scope to a clear manifestation of reinforcement characteristics from elastic to plastic and finally with fracture after necking. The cyclic test results of beam specimens with STMT reinforcement are shown in Figs. 5(c) and 5(d). The yield points are also observed but ductility is reduced to about 3.0. The resulting failure is similar to the pushover tests but major flexural cracks form on both faces of the beam, finally leading to fracture of reinforcing bars. There is a clear manifestation of reinforcement characteristics from elastic to plastic, and finally with a sign of brittle fracture due to breaking of reinforcement at failure.

The pushover results of beam specimens with LTMT reinforcement are shown in Figs. 6(a) and 6(b). The yield point is observed in both the results of this type of reinforcement with a large difference in ductile pattern. The failure pattern of beam specimens with LTMT reinforcement is the same as in the previous case. The cyclic results of LTMT reinforcement beams are shown in Figs. 6(c) and 6(d) which also manifests the yield point, but the ductility is equal or greater than 6. The resulting failures of beam specimens are in the form of development of flexural cracks on both the faces that finally lead to fracture of reinforcing bars. A large variation in strength is observed in the beam specimens. The effect of variation in specified nominal yield may lead to variation in design strength which results in variation in failure load. Hence, complete characteristics of the reinforcement involved in the construction need to be known.

The pushover test results of beam specimens with TOR reinforcement are shown in Figs. 7(a) and 7(b). The typical behavior of nonspecific yield type reinforcement is observed in both the results, i.e., with the absence of a distinct yield point. The specimens show very limited ductile behavior. Failure is initiated with formation of major flexural cracks at localized area of the applied load, which finally lead to sequential fracture of reinforcing bars. Failure patterns of the specimens clearly reflect brittle sequential fracture of the reinforcing bars. The cyclic test results of TOR reinforcement beams are shown in Figs. 7(c) and 7(d). The yield point is not observed and ductility is reduced to about 2.7. The resulting failure is similar to those in the pushover tests except major flexural cracks form on both faces of the beam leading to fracture of reinforcing bars.

4 Comparative performance of beam specimens with different characteristics of reinforcing bars

A comparative study is also carried out on beam specimens in order to evaluate the effect of number of experimental and constructional parameters. The discussion of the test results is as follows.

4.1 Under varied ρ% but with similar reinforcement & similar loading types

The comparative performance of beam specimens with STMT reinforcement is shown in Fig. 8 (a) under

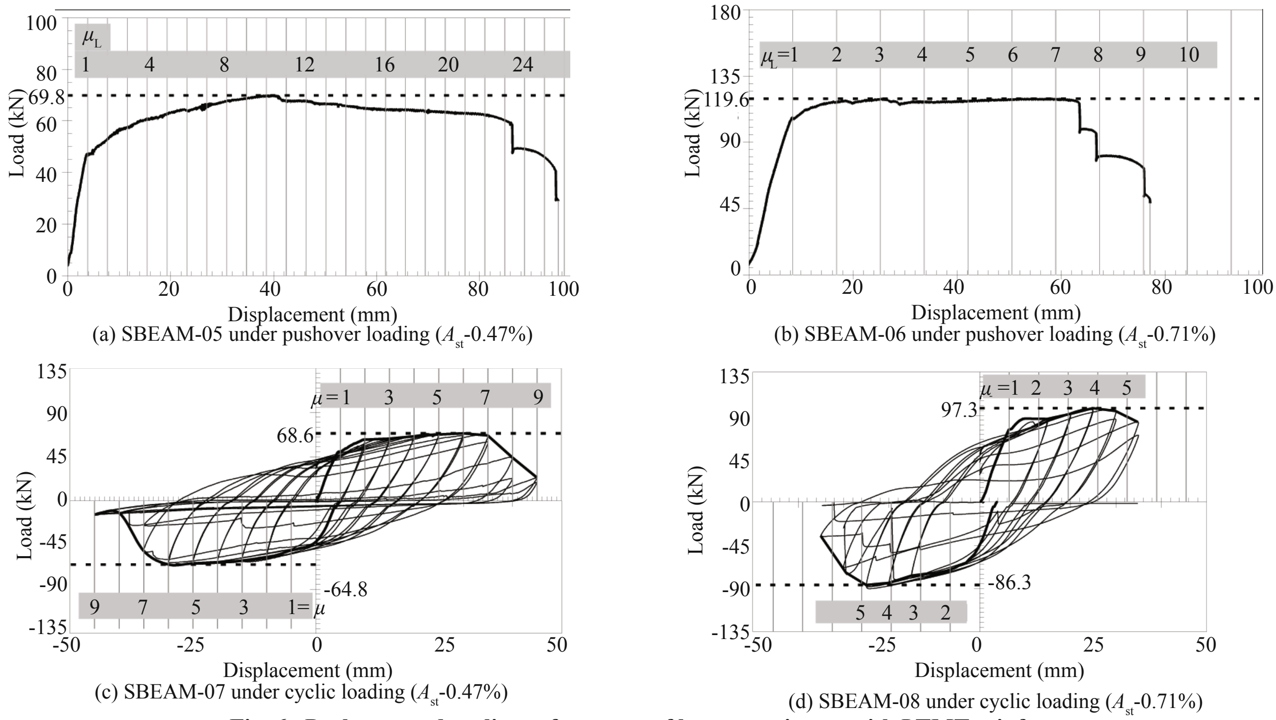

(a) SBEAM-05 under pushover loading (A_{st}-0.47%)
(b) SBEAM-06 under pushover loading (A_{st}-0.71%)
(c) SBEAM-07 under cyclic loading (A_{st}-0.47%)
(d) SBEAM-08 under cyclic loading (A_{st}-0.71%)

Fig. 6 Pushover and cyclic performance of beam specimens with LTMT reinforcement

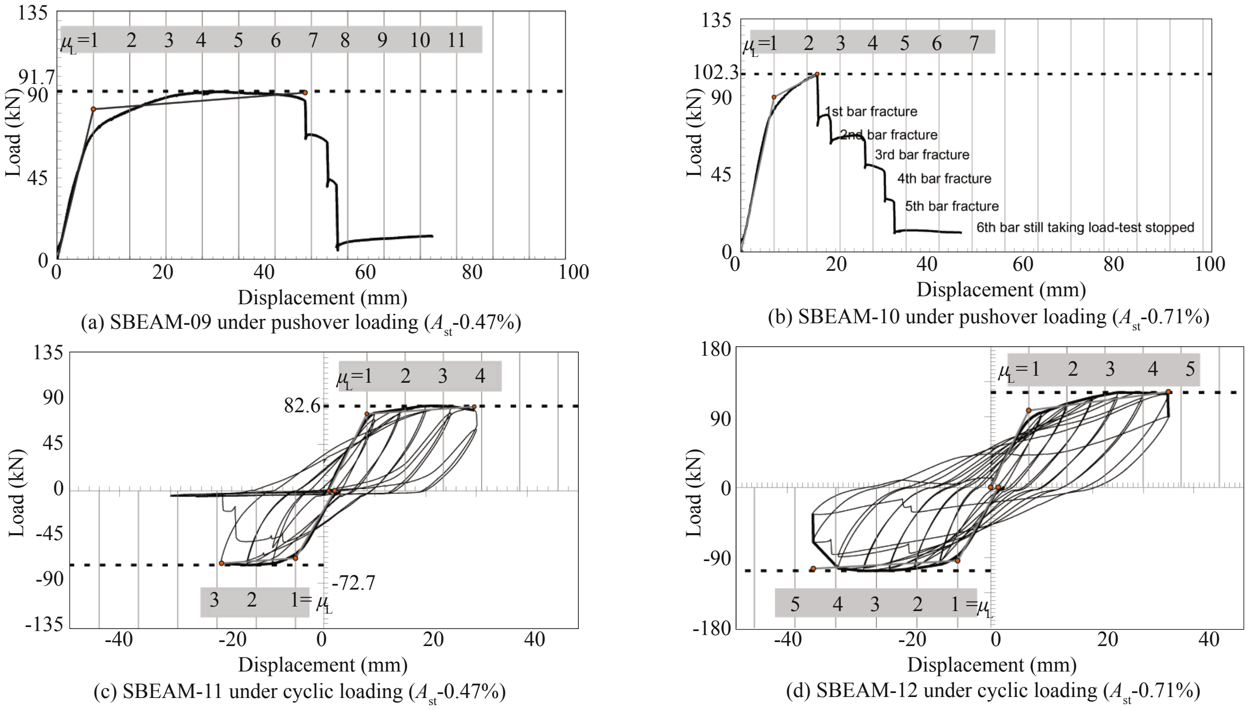

(a) SBEAM-09 under pushover loading (A_{st}-0.47%)
(b) SBEAM-10 under pushover loading (A_{st}-0.71%)
(c) SBEAM-11 under cyclic loading (A_{st}-0.47%)
(d) SBEAM-12 under cyclic loading (A_{st}-0.71%)

Fig. 7 Pushover and cyclic performance of beam specimens with TOR reinforcement

pushover and cyclic loading. It is observed that the strength increases and the overall deformation capacity also increases under pushover and cyclic loading as the percentage of reinforcement increases. Similarly, the comparative performances of beam specimens with LTMT reinforcement and TOR reinforcement are shown in Fig. 8(b) and Fig. 8(c), respectively. It is observed that an increase in % of reinforcement helps to increase the strength only, but the ductile response is not affected significantly.

4.2 Under similar ρ% & loading, but with varied reinforcement types

The comparative performances of beam specimens with different types of reinforcement of equal percentage,

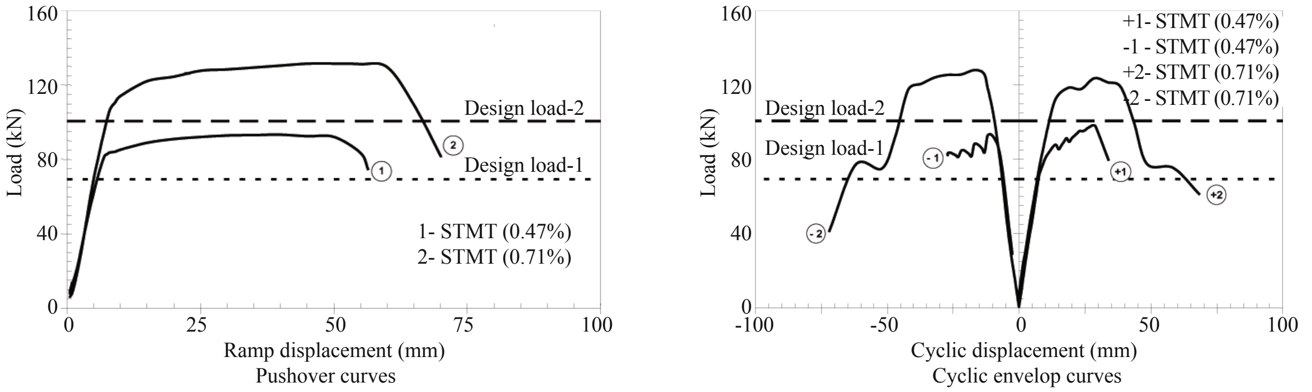

(a) Comparisons of beam specimens with STMT reinforcement

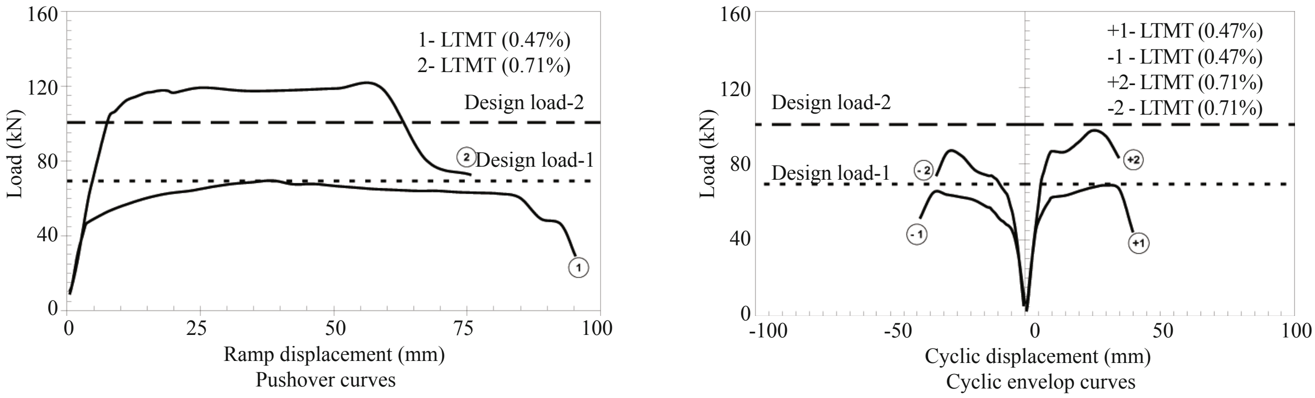

(b) Comparisons of beam specimens with LTMT reinforcement

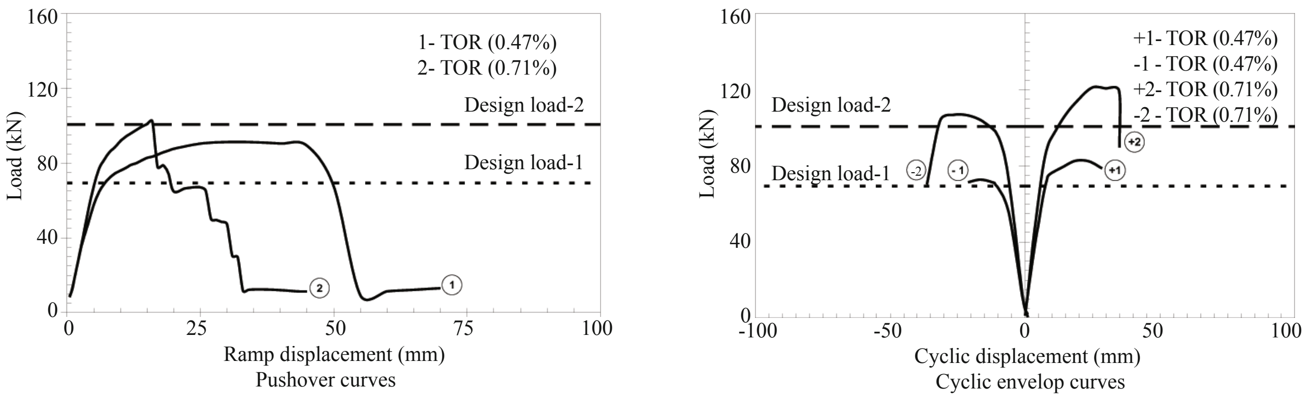

(c) Comparisons of beam specimens with TOR reinforcement

Fig. 8 Comparisons of pushover and cyclic envelope curve of beam specimens of different types of reinforcement (a) STMT (b) LTMT (c) TOR

i.e., 0.47% & 0.71%, under pushover and cyclic loading are shown in Fig. 9 and Fig. 10, respectively. It is clearly evident that beam specimens with STMT reinforcement under either pushover loading or cyclic loading sustain maximum load and deformation as compared to specimens with other types of reinforcement. The pushover and cyclic performance of beam specimens with LTMT reinforcement exhibits no obvious trend. The pushover curves of beam specimens with TOR reinforcement show sudden brittle failure as compared to beam specimens with STMT reinforcement.

4.3 Under varied ρ% & varied loading but with similar reinforcement types

The comparative performance of beam specimens with different types of reinforcement under pushover and cyclic loading are shown in Fig. 11. It is evident that the type of loading is a more pronounced factor for the determination of load-deformation characteristics of any RC component. There is a large variation in strength and ductility parameters of beam specimens evaluated under pushover loading and cyclic loading. There is a

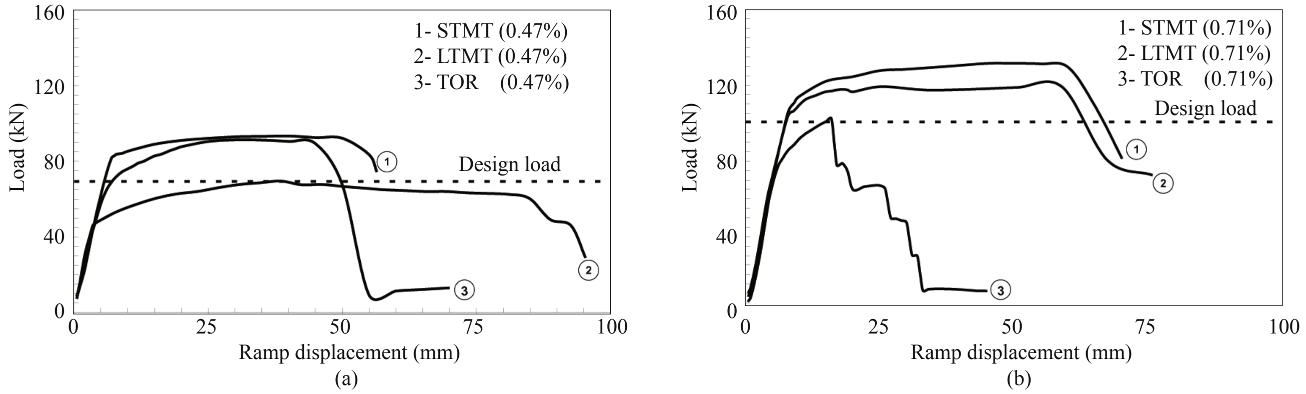

Fig. 9 Comparisons of pushover envelope curve of beam specimens with equal percentage of reinforcement (a) 0.47% (b) 0.71%

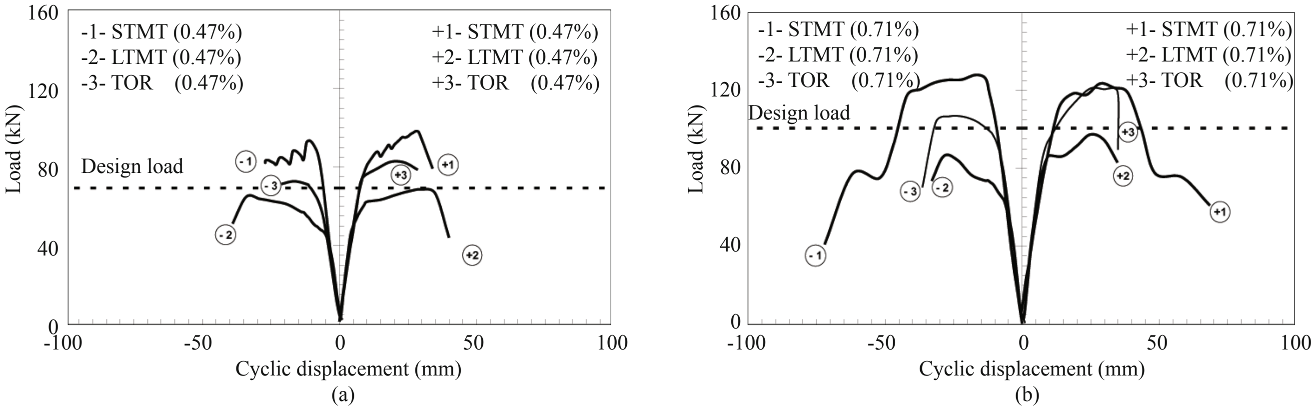

Fig. 10 Comparisons of cyclic envelope curve of beam specimens with equal percentage of reinforcement (a) 0.47% (b) 0.71%

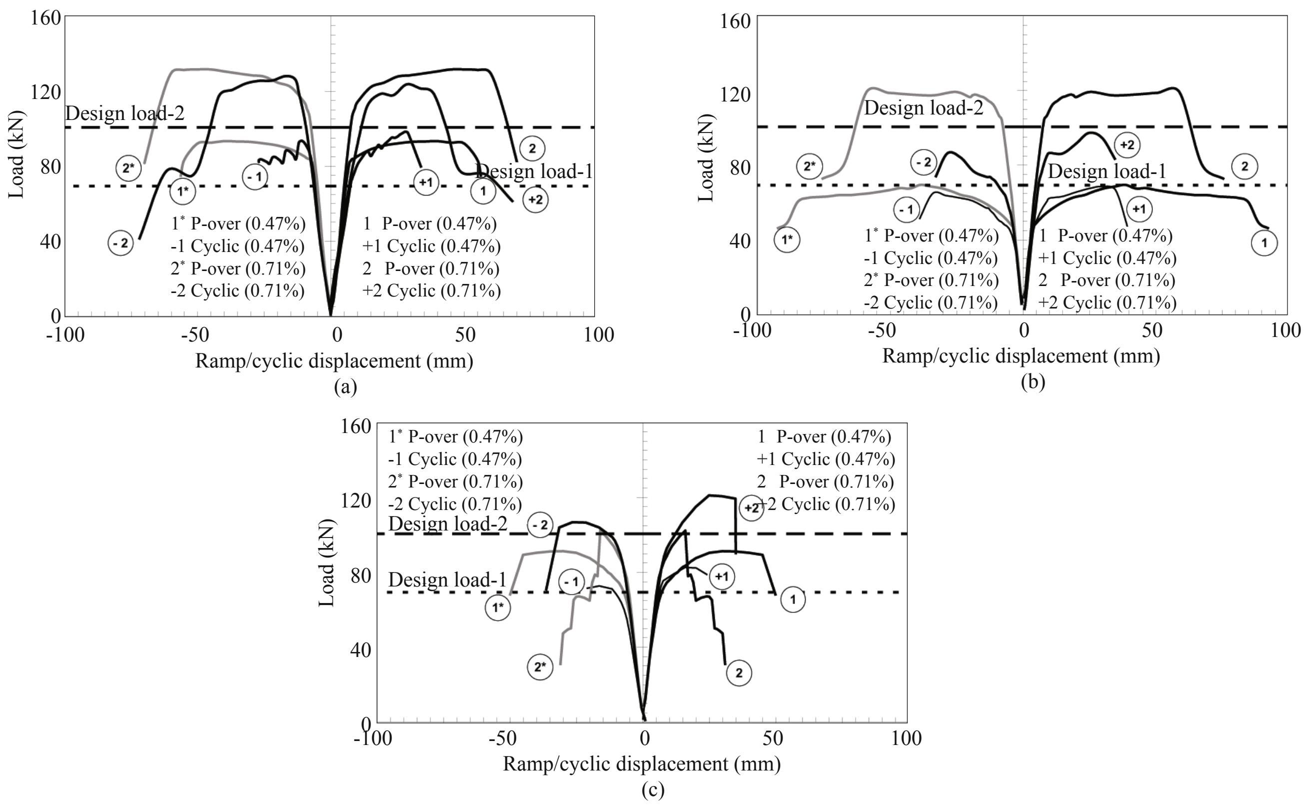

Fig. 11 Comparison of pushover curves vs. envelop of hysteresis curves of beam specimens of varying % of reinforcement of different types (a) STMT (b) LTMT (c) TOR

significant decrease in deformation capacities under cyclic loading as compared to pushover loading. The type of reinforcement also has a predominant effect on the deformation capacity of beams.

4.4 Under the energy dissipation capacity

The energy dissipation of the beam specimens with different types of reinforcement under pushover and cyclic loading is shown in Fig. 12. Beam specimens with STMT reinforcement have much higher energy dissipation as compared to other types of reinforcement. Lesser energy dissipation is observed in specimens with TOR reinforcement. This pattern is observed in pushover or cyclic testing of beam specimens, with both % of reinforcements.

4.5 Under the strength and stiffness degradation

Strength and stiffness degradation over the yield strength and yield stiffness of the beam specimens are evaluated and compared in Fig. 13. The reduction of resistance (degradation of strength and stiffness) is mainly due to reduction in moment of inertia or cross sectional area because of propagation of cracking with increasing displacement load history, either in pushover testing or cyclic testing. The upper bunch of curves represents the post elastic stiffness degradation in % and the lower bunch of curves represents the post elastic strength degradation in %. It is evident that stiffness degradation of beam specimens with STMT reinforcement is less as compared to specimens with LTMT and TOR reinforcement**.** It is also evident that the initial trend of stiffness degradation of beam specimens is nearly the same either in the case of cyclic loading or pushover loading. There is no significant loss of strength after yielding of beam specimens constructed with different types of reinforcement. The specimens also represent an over-strength factor which depends upon the strain hardening effect of respective reinforcement.

5 Evaluation of plastic rotation capacity of beam specimens with different characteristics of reinforcing bars

The plastic rotations are useful for modeling the nonlinear component deformation capacities of structure under seismic performance evaluations. The experimental plastic rotation (θ_p) is defined as the difference between the ultimate rotation (θ_U) and the rotation at yielding (θ_Y). The rotation at yielding is evaluated by idealizing the moment-rotation relationship obtained from pushover and cyclic testing of beam specimens with different types of reinforcement as shown in Fig. 14. The ultimate rotation is taken as the rotation corresponding to a residual (reduced) strength of about 80% of maximum load (or 20% drop of maximum strength) responsible for flexural failure of the beams.

As per ASCE/SEI 41-06, the force-deformation curves are modified as idealized force-deformation curves for computer modeling and acceptance criteria for deformation-controlled actions so that force–deformation curves are converted to normalized force (Q/Q_y) versus deformation (θ or Δ) with the parameters *a*, *b* and *c* or normalized force (Q/Q_y) versus deformation ratio (θ/θ_y, Δ/Δ_y, Δ/h) with the parameters *d*, *e* and *c* as shown in Figs. 15(a) and 15(b). Elastic stiffness and the values for the parameters *a, b, c, d* and *e* are used to define the acceptance criteria for Primary (P) and Secondary (S) components. The most common acceptance criteria are Immediate Occupancy (IO), Life Safety (LS) and Collapse Prevention (CP) as shown in Fig. 15(c).

As per ASCE/SEI 41-06, for beams controlled by flexure, the following controlling parameters are defined as below;

(i) The ratio of the difference of tension (ρ) & compression steel (ρ') to balanced steel (ρ_{bal}) i.e. $\left(\frac{\rho-\rho'}{\rho_{bal}}\right)$ in the limiting range of (≤ 0 and ≥ 0.5).

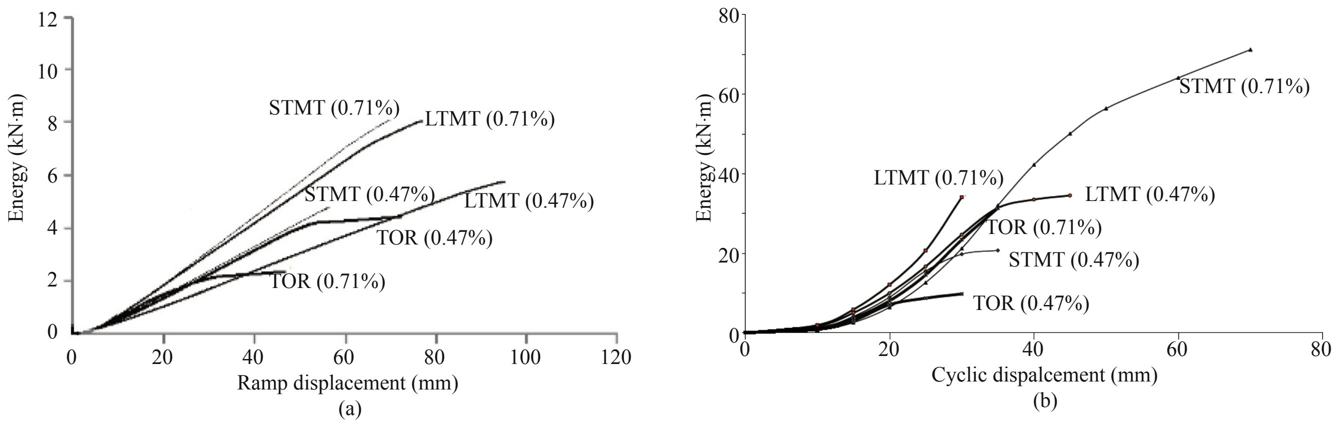

Fig. 12 Cumulative dissipation of energy in the formation of plastic hinges in beam specimens with different types of reinforcement under (a) pushover loading (b) cyclic loading

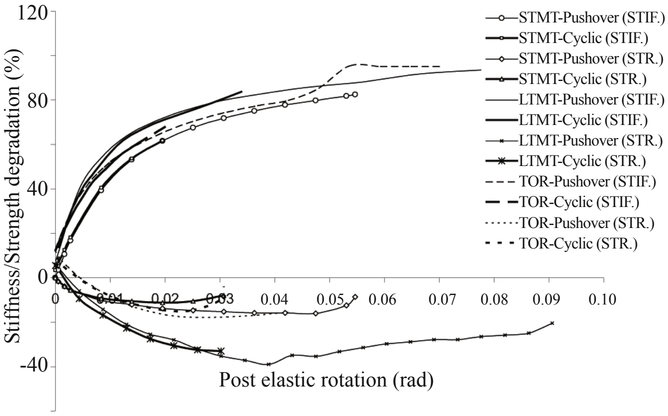

Fig. 13 Post elastic strength and stiffness degradation over yield in beam specimens with different types of reinforcement

In the present study, the ratio of the difference of tension (ρ) & compression steel (ρ') to balanced steel (ρ_{bal}) i.e. $(\rho-\rho')/(\rho_{bal})$ is in the limiting range of ($\leq$ 0), as all the tested beams are with equal tension and compression reinforcements.

(ii) Condition of transverse reinforcement confinement i.e. Confirming "C" and Non-confirming "NC"

In the present study, all the beam specimens come under non-conforming condition ("NC") since d/3 ratio for short beam specimens is 82 mm while $d_{provided}$ = 180 mm.

(iii) Ratio of nominal shear stress to square root of compressive stress of concrete i.e. $\left(\dfrac{V}{b_w d\sqrt{f_c'}}\right)$ under two limits i.e. ≤ 3 and ≥ 6. Where, V is the shear strength and is considered under two concepts (i) based on flexure capacity and (ii) shear capacity of section reinforcement as per IS 456: 2000 (2000) and obtained as, $V = V_c + V_S = \tau_c bd + \dfrac{d}{x} A_{SV}\, 0.87 f_y$, where, A_{SV} is the area of vertical stirrups, τ_c is the design shear strength of concrete, f_y is the nominal yield strength of shear stirrups, x is the spacing of vertical stirrups with b and d being breadth and effective depth of beam section. b_w is the width and d is the effective depth of beam.

The ratios correspond to beam specimens 0.47% and 0.71% reinforcement is 3.8 and 4.2 respectively.

Based on the above mentioned controlling parameters, the nonlinear modeling parameter "a" for flexural failure condition of all the beam specimens are evaluated in Table 2 by interpolation of the values given in ASCE/SEI 41-06. The values as compared to experimentally obtained values with different types of reinforcements (STMT, LTMT, and TOR) are shown in Fig. 16. It may be concluded that the type of reinforcement is a significant parameter on which the Force–Deformation relationship of an RC component depends.

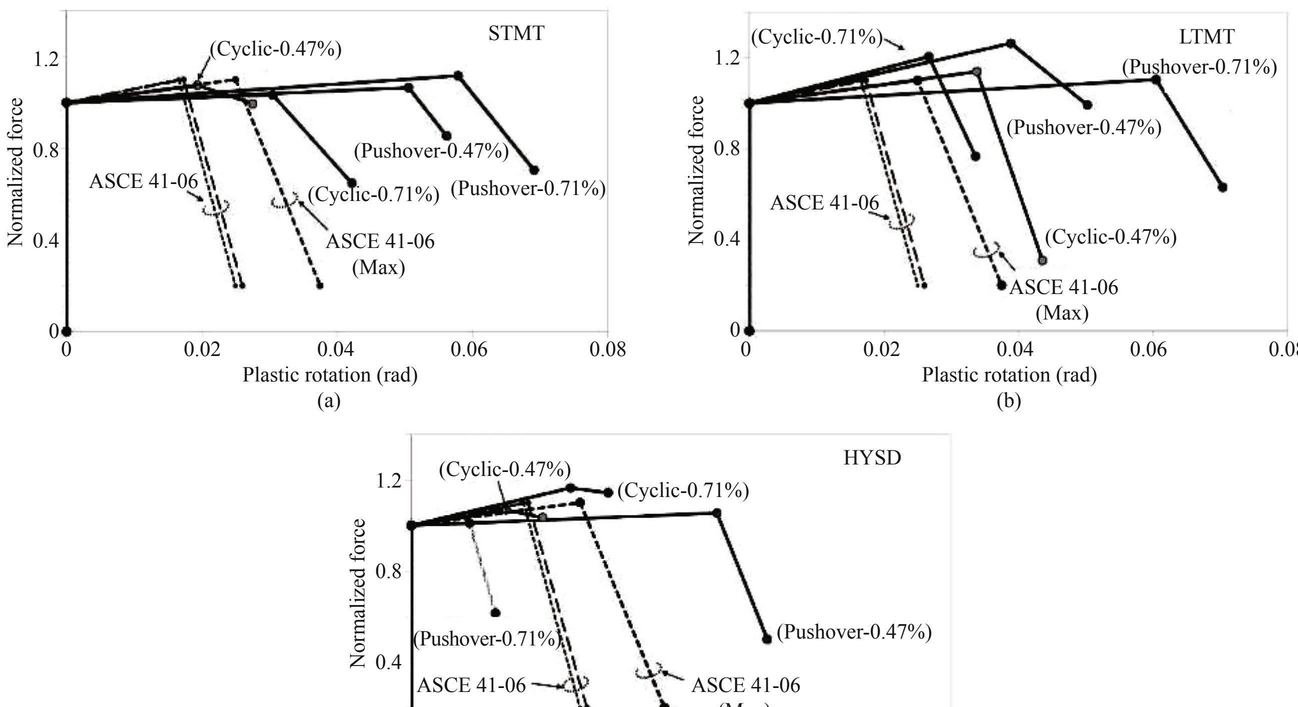

Fig. 14 Moment rotation relationship obtained from pushover and cyclic testing of beam specimens in different types of reinforcement (a) STMT (b) LTMT and (c) TOR

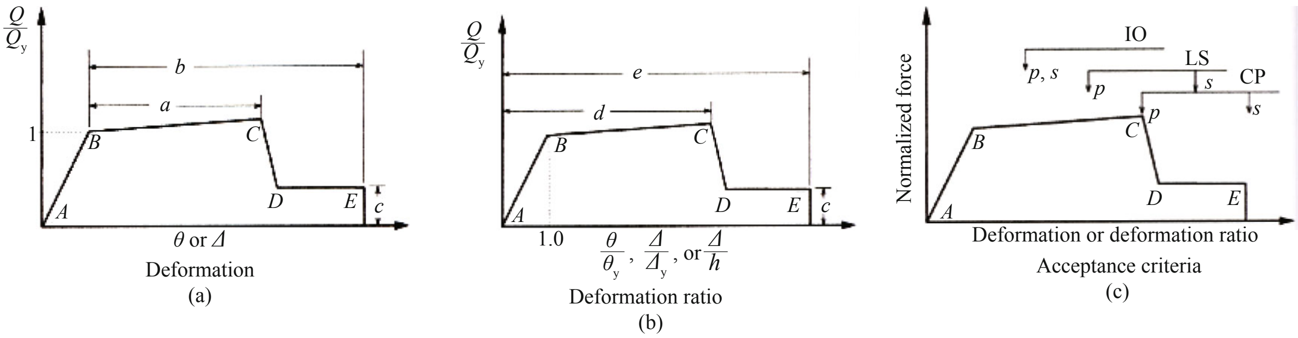

Fig. 15 Generalized force – deformation relations for RC components for modeling and acceptance criteria (ASCE/SEI 41-06, 2007)

Table 2 Experimental obtain non-linear modeling parameter "*a*" for the beam specimens with different types of reinforcement under pushover and cyclic testing

SBEAM types		Plastic rotations (radians)				Ratios of plastic rotations				
				ASCE/SEI 41-06						
	A_{st}(%)	Pushover	Cyclic	(Flex. Cond.)	(Max.)	Pushover			Cyclic	
		(i)	(ii)	(iii)	(iv)	(i)/(ii)	(i)/(iii)	(i)/(iv)	(ii)/(iii)	(ii)/(iv)
STMT	0.47	0.051	0.0195	0.017	0.025	2.62	3.0	2.04	1.15	0.78
	0.71	0.058	0.0305	0.017	0.025	1.90	3.4	2.32	1.80	1.22
LTMT	0.47	0.088	0.032	0.017	0.025	2.75	5.17	3.52	1.90	1.28
	0.71	0.061	0.025	0.017	0.025	2.44	3.60	2.44	1.47	1.0
TOR	0.47	0.046	0.015	0.017	0.025	3.07	2.70	1.84	0.9	0.6
	0.71	0.019	0.031	0.017	0.025	0.61	1.17	0.76	1.82	1.24

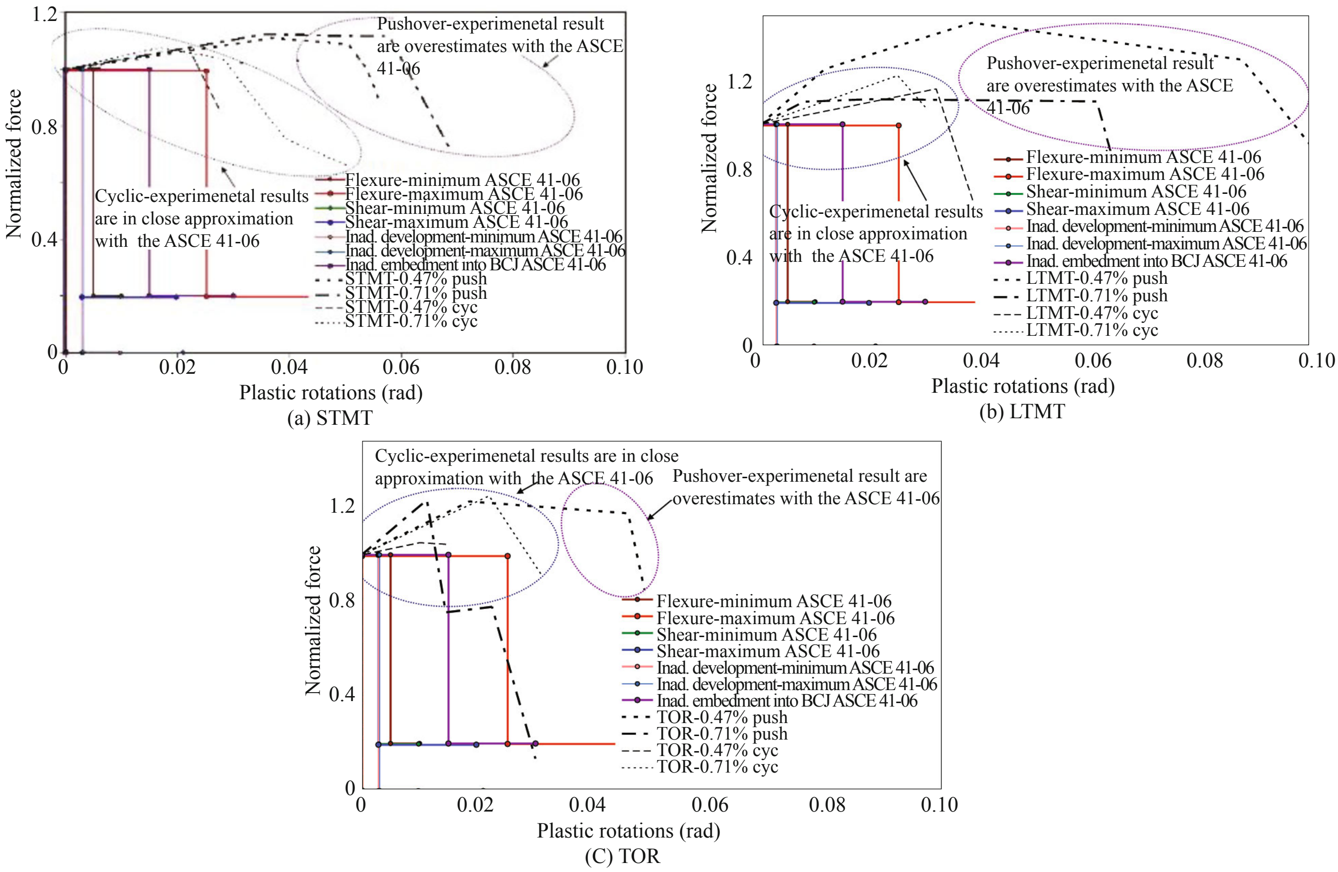

Fig. 16 Comparison of nonlinear plastic hinge parameter "*a*" of beam specimens under different reinforcement (a) STMT (b) LTMT and (c) TOR with the ASCE/SEI 41-06 prescribed values

6 Conclusions

(1) The load-deformation pushover curves of beam specimens with STMT and LTMT reinforcements reflect a ductile performance in their behavior by depicting clear yield point with 1.12 over strength factor and approximately the same amount of ductility. The pushover curves of beam specimens with TOR reinforcement do not reflect any specific yield of reinforcement and show a brittle failure with comparatively low ductility as well as energy dissipation. The load-deformation pushover curves of beam specimens under two different characteristics of reinforcement clearly depict difference in ductile performance. Therefore, the nonlinear plastic hinge properties have to be updated on the basis of types of reinforcement.

(2) Cyclic load-deformation curves of beam specimens reflect similar strength attainment, but with reduced ductility as compared to pushover loading. Beam specimens with STMT/ LTMT reinforcement exhibit ductile behavior and also more energy dissipation as compared to beam specimens in TOR reinforcement. Therefore, for seismic performance evaluations, the nonlinear hinge properties obtained from pushover tests have to be modified on the basis of experimental investigations.

(3) The energy dissipation ratio of beam specimens obtained from the envelope of cyclic hysteretic diagram to load-deformation pushover curve for beam specimens vary from 0.4 to 1.0 depending upon the type and % of TMT reinforcement. The energy dissipation ratio obtained from the cyclic hysteresis diagram i.e. total energy dissipation in all the cycles to fail the specimens to its envelope of cyclic hysteretic diagram becomes 2.5 to 5.0. Low energy dissipation is observed in beam specimens with TOR reinforcement under pushover and cyclic testing. Therefore, it is conferred that pushover curve represents the approximate actual strength of the specimens but higher ductility and also manifests lower energy dissipation as compared to its cyclic counterpart.

(4) Evaluated plastic rotations parameters clearly manifest the effect of types of reinforcement. The values of plastic rotation are much smaller in case of brittle type of reinforcement (TOR) as compared to ductile type of reinforcement (TMT). This is important particularly in case of assessment and evaluation of old buildings which are generally constructed in TOR reinforcement while recent construction is in TMT reinforcement. It is also observed that the variation in nonlinear parameters is not significant in the same nature of reinforcements such as STMT, LTMT. It may be concluded that the type of reinforcement is a significant parameter on which the Force–Deformation relationship of an RC component depends.

(5) The values of nonlinear plastic hinge parameters as suggested by ASCE/SEI 41-06 (2007) are closer to values obtained from the cyclic testing of specimens. The values obtained from the specimens in TOR reinforcement lie in between the prescribed values of ASCE/SEI 41-06 (2007). It seems reasonable that the testing in the past has generally been carried out on brittle type of reinforcement or deformed type of reinforcement while the TMT type of reinforcement is a recent development and hence the properties are to be modified based on reinforcement in use.

(6) Nonlinear hinge modeling parameter obtained from the pushover testing is approximately 2 to 3 times higher than the values obtained from cyclic testing. The experimentally observed values of the parameters under cyclic tests of beam specimens with STMT and LTMT reinforcement are closer to maximum recommended values in ASCE/SEI 41-06 (2007).

References

ASCE/SEI 41–06 (2007), *Seismic Rehabilitation of Existing Buildings*, ASCE Standard, American Society of Civil Engineers, Reston: USA.

Caripinteri A, Corrado M, Paggi M and Mancini G (2009), "New Model for the Analysis of Size-scale Effects on the Ductility of Reinforced Concrete Elements in Bending," *Journal of Engineering Mechanics*, **135**(3): 221–229.

Darwin D and Nmai CK (1986), "Energy Dissipation in RC Beams under Cyclic Load," *Journal of the Structural Division*, **112**(8): 1829–1846.

Fantilli AP, Ferretti D and Rosati G (2005), "Effect of Bar Diameter on the Behavior of Lightly Reinforced Concrete Beams," *Journal of Materials in Civil Engineering*, **17**(1): 10–18.

Haskett M, Oehlers DJ and Ali M.SM and Wu C (2009), "Yield Penetration Hinge Rotation in Reinforced Concrete Beams," *Journal of Structural Engineering*, **135**(2): 130–138.

Hwang T and Scribner CF (1984), "R/C Member Cyclic Response during Various Loadings," *Journal of the Structural Division*, **110**(3): 477–489.

Inel M and Ozmen HB (2006), "Effects of Plastic Hinge Properties in Nonlinear Analysis of Reinforced Concrete Buildings," *Engineering Structures*, **28**: 1494–1502.

IS 13920: 1993 (1993), *Indian Standard Ductile Detailing of Reinforced Concrete Structures Subjected to Seismic Forces–Code of Practice*, Bureau of Indian Standard, India.

IS 456: 2000 (2000), *Indian Standard Plain and Reinforced Concrete Code of Practice*, Fourth Revision, Bureau of Indian Standard, India.

Iyengar KTSR, Desayi P and Reddy KN (1972), "Confined Concrete–Its Application in R.C. Beams and Frames," *Building Science*, **7**(8): 105–120.

Marefat MS, Shirazi SMH, Rostamshirazi R and Khanmohammadi M (2009), "Cyclic Response of Concrete Beams Reinforced by Plain Bars," *Journal of*

Earthquake Engineering, **13**: 463–481.

Marfia S, Rinaldi Z and Sacco E (2004), "Softening Behavior of Reinforced Concrete Beams under Cyclic Loading," *International Journal of Solids and Structures*, **41**: 3293–3316.

Melo J, Fernandes C, Varum H, Rodrigues H, Costa A and Arede A (2011), "Numerical Modeling of the Cyclic Behavior of RC Elements Built with Plain Reinforcing Bar," *Engineering Structures*, **33**: 273–286.

Oehlers DJ, Liu IST and Seracino R (2005), "The Gradual Formation of Hinges throughout Reinforced Concrete Beams," *Mechanics Based Design of Structures and Machines*, **33**(3): 373–398.

Scott RH and Whittle RT (2005), "Moment Redistribution Effects in Beams," *Magazine of Concrete Research*, **57**(1): 9–20.